Metabolic Engineering xxx (xxxx) xxx

Contents lists available at ScienceDirect

Metabolic Engineering

journal homepage: www.elsevier.com/locate/meteng

Constructing an ethanol utilization pathway in *Escherichia coli* to produce acetyl-CoA derived compounds

Hong Liang [a,b], Xiaoqiang Ma [a], Wenbo Ning [b], Yurou Liu [a,b], Anthony J. Sinskey [a,c], Gregory Stephanopoulos [a,d,**], Kang Zhou [a,b,*]

[a] Disruptive & Sustainable Technologies for Agricultural Precision (DiSTAP), Singapore-MIT Alliance for Research and Technology, Singapore
[b] Department of Chemical and Biomolecular Engineering, National University of Singapore, Singapore
[c] Department of Biology, Massachusetts Institute of Technology, United States
[d] Department of Chemical Engineering, Massachusetts Institute of Technology, United States

ARTICLE INFO

Keywords:
Ethanol utilization pathway
E. coli
Acetyl-CoA
Polyhydroxybutyrate
Metabolic engineering

ABSTRACT

Engineering microbes to utilize non-conventional substrates could create short and efficient pathways to convert substrate into product. In this study, we designed and constructed a two-step heterologous ethanol utilization pathway (EUP) in *Escherichia coli* by using acetaldehyde dehydrogenase (encoded by *ada*) from *Dickeya zeae* and alcohol dehydrogenase (encoded by *adh2*) from *Saccharomyces cerevisiae*. This EUP can convert ethanol into acetyl-CoA without ATP consumption, and generate two molecules of NADH per molecule of ethanol. We optimized the expression of these two genes and found that ethanol consumption could be improved by expressing them in a specific order (*ada-adh2*) with a constitutive promoter (PgyrA). The engineered *E. coli* strain with EUP consumed approximately 8 g/L of ethanol in 96 h when it was used as sole carbon source. Subsequently, we combined EUP with the biosynthesis of polyhydroxybutyrate (PHB), a biodegradable polymer derived from acetyl-CoA. The engineered *E. coli* strain carrying EUP and PHB biosynthetic pathway produced 1.1 g/L of PHB from 10 g/L of ethanol and 1 g/L of aspartate family amino acids in 96 h. We also engineered a *E. coli* strain to produce 24 mg/L of prenol in an ethanol-containing medium, supporting the feasibility of converting ethanol into different classes of acetyl-CoA derived compounds.

1. Introduction

With the increasing concerns over climate change and greenhouse gas emissions, the production of fuels and chemicals from renewable feedstock by using engineered microbes has been considered to be a promising way of reducing the chemical industry's carbon footprint (Whitaker et al., 2017). The feedstock usually needs to be assimilated into central carbon metabolism of the microbes, which provides (1) building blocks for the synthesis of the needed enzymes (biocatalysts), (2) substrates of product formation, and (3) the needed energy (Protzko et al., 2018). Microbes used in such processes typically utilize sugars, fatty acids, and/or organic acids as the carbon sources (Wendisch et al., 2016). To date, extensive work has been done to explore short and more carbon-efficient assimilation pathways to synthesize acetyl-CoA, a key compound in the central metabolism, and the precursor of many value-added acetyl-CoA derived compounds, such as vitamins, fragrance/flavor molecules, and pesticides (Lian et al., 2014).

The shortest biosynthetic pathway of acetyl-CoA starts with acetate, which requires one enzymatic step, but consumes at least one ATP per acetyl-CoA (Lian et al., 2014; Liu et al., 2019). During the assimilation of acetate, pH would increase, thus complicating the fermentation process, especially at the shake flask scale. In comparison with acetate, ethanol is a neutral molecule and will not change the pH when it is consumed. Compared with glucose or other substrates (Bang and Lee, 2018; Fuhrer et al., 2005; Woolston et al., 2018), which often need many complex steps to generate acetyl-CoA, ethanol can be converted into acetyl-CoA in shorter enzymatic steps. Ethanol can be acquired from renewable sources through a number of processes. Currently,

* Corresponding author. Disruptive & Sustainable Technologies for Agricultural Precision (DiSTAP), Singapore-MIT Alliance for Research and Technology, Singapore.
** Corresponding author. Disruptive & Sustainable Technologies for Agricultural Precision (DiSTAP), Singapore-MIT Alliance for Research and Technology, Singapore.
E-mail addresses: gregstep@mit.edu (G. Stephanopoulos), kang.zhou@nus.edu.sg (K. Zhou).

https://doi.org/10.1016/j.ymben.2020.11.010
Received 22 May 2020; Received in revised form 30 October 2020; Accepted 15 November 2020
Available online 25 November 2020

many countries are making efforts to develop cost-effective processes to produce ethanol from renewable biomass, such as cellulosic hydrolysates of crop residues (Robak and Balcerek, 2018). It could be economically feasible to produce acetyl-CoA derived compounds from the biomass-derived ethanol (Fig. 1a) if the yield of the targeted compounds from ethanol is much higher than that of using glucose, a commonly used carbon source in the industry. Carbon dioxide (CO_2) is the most prevalent greenhouse gas emitted by humans' activities. Compared with the multiple steps of natural plant-based CO_2 assimilation, alternative ways of turning CO_2 into one- and two-carbon chemicals in one-step have been extensively explored (Fig. 1a). Methanol (Gurudayal et al., 2017), formate (Yadav et al., 2012), ethanol (Ren et al., 2015; Song et al., 2016) and acetate (Sakimoto et al., 2016) have been produced from CO_2 by using hydrogen or electricity as the source of energy. Among them, electrochemically converting CO_2 into ethanol has received extensive attention from the catalysis community recently (Arán-Ais et al., 2020; Li et al., 2019; Luo et al., 2019; Ma et al., 2020; Ting et al., 2020). With further technological development, the CO_2-derived ethanol may become an abundant, renewable, and affordable substrate to fuel the ethanol-based fermentation processes.

Escherichia coli is a well-studied model microorganism and plays a critical role in the modern fermentation industry. Many genetic tools have been developed for *E. coli* to produce valuable small molecules and recombinant proteins at high titers (Pontrelli et al., 2018). *E. coli*, however, is naturally incapable of metabolizing ethanol at a sufficient rate to support cell growth (Fig. 1b). Herein, we introduced a two-step ethanol utilization pathway (EUP) in *E. coli* to produce polyhydroxybutyrate (PHB), an acetyl-CoA derived product. With metabolic engineering, the engineered *E. coli* strain grew on ethanol as the sole carbon source and produced 1.1 g/L of PHB from 10 g/L of ethanol in 96 h with supplementation of small amount of amino acids. To further expand the scope of acetyl-CoA derived compounds from ethanol, we coupled the EUP developed in this study with a prenol biosynthetic pathway. The engineered *E. coli* strain produced 24 mg/L of prenol in a medium containing 10 g/L of ethanol in 48 h. Collectively, these results proved the usefulness of employing EUP to produce value-added acetyl-CoA derived chemicals in *E. coli*.

2. Materials and methods

2.1. Chemicals

All the chemicals were purchased from Sigma-Aldrich unless specifically mentioned. DNA oligonucleotides used in this work were synthesized by Integrated DNA Technologies.

2.2. Plasmids and strain construction

Plasmids were constructed according to the Guanin/Thymine standard (Ma et al., 2019). The constructed plasmids were verified by sequencing (service provider: Bio Basic Asia Pacific Pte Ltd, Singapore). Each of the constructed plasmids was introduced into *E. coli* **MG1655_DE3** (*ΔrecA, ΔendA, DE3*), **MG1655_DE3_ΔaldB** (*ΔrecA, ΔendA, ΔaldB, DE3)* or **BL21_DE3** (New England Biolabs, C2527H) via the standard electroporation protocol (Ma et al., 2019). The successfully constructed strains were then isolated on Luria Bertani (LB) agar plate containing proper antibiotics. All the strains used in this study are summarized in Table 1.

2.3. E. coli genome editing

A previously reported CRISPR-Cas9 system (Jiang et al., 2015) was used to delete *aldB* (coding $NADP^+$-dependent aldehyde dehydrogenase) or *pta* (phosphate acetyltransferase) in the genome of *E. coli* **MG1655-DE3**.

2.4. Cell culture and medium

To prepare the seed culture of *E. coli*, a single colony picked from a LB agar plate was inoculated into 10 mL of LB medium containing proper antibiotics and grown at 37 °C/220 rpm overnight. The overnight culture was inoculated (1%, v/v) into a chemically defined medium, K3 medium (Zhou et al., 2015). Culture volume and vessel size of every experiment are specified in caption of the associated figures. The subsequent cell culture processes were done at 30 °C/220 rpm. The K3 medium composition (working concentration): 13.3 g/L KH_2PO_4, 4 g/L

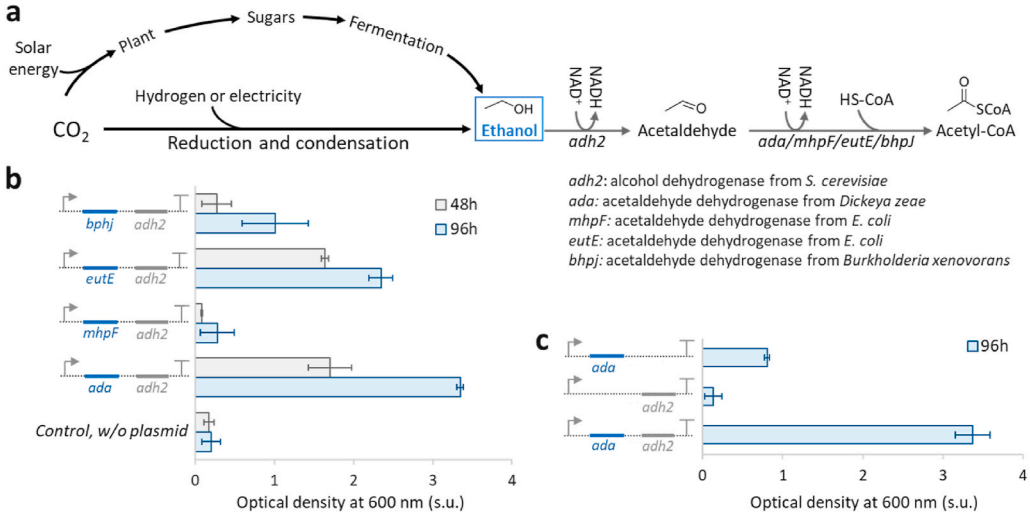

Fig. 1. Construction of a two-step ethanol utilization pathway (EUP) in *E. coli*. (**a**) Schematic of the EUP and potential sources of ethanol. (**b**) Screening four acetaldehyde dehydrogenases based on OD600. The strains used from top to bottom were **PthrC3_BH**, **PthrC3_EH**, **PthrC3_MH**, **PthrC3_AH**, **MG1655_DE3**. More information of the *E. coli* strains can be found in Table 1. Accession numbers of the enzymes: NCBI WP_012885841 (Ada), UniProt P77580 (MhpF), NCBI WP_104208495 (EutE), NCBI WP_020206178 (BhpJ), and NCBI NP_014032 (Adh2). (**c**) Testing if both genes of EUP were essential. The strains used here were **PthrC3_A**, **PthrC3_H** and **PthrC3_AH** (from top to bottom). Cells were cultured at 30 °C using 10 g/L of ethanol as the sole carbon source (no amino acids or nucleobases supplemented). Culture volume and vessel size: 10 mL of culture in 50 mL tubes. Promoter PthrC3 was used in all the *E. coli* strains to overexpress the gene(s). s.u.: standard unit. Error bars indicate standard error (n = 3).

Table 1
Strains and plasmids used in this study.

Strain name	Genotype of plasmid(s) carried by the strain	Applications in this study
PthrC3_BH	*PthrC3_bphj_adh2_pMB1_AmpR* (Plasmid EUPp_01)	Screening acetaldehyde dehydrogenase for EUP
PthrC3_EH	*PthrC3_eutE_adh2_pMB1_AmpR (Plasmid EUPp_02)*	Screening acetaldehyde dehydrogenase for EUP
PthrC3_MH	*PthrC3_mhpF_adh2_pMB1_AmpR (Plasmid EUPp_03)*	Screening acetaldehyde dehydrogenase for EUP
PthrC3_AH	*PthrC3_ada _adh2_pMB1_AmpR (Plasmid EUPp_04)*	Screening acetaldehyde dehydrogenase for EUP
PthrC3_AH6	*PthrC3_ada _adh6_pMB1_AmpR (Plasmid EUPp_05)*	Screening alcohol dehydrogenase for EUP
PthrC3_HA	*PthrC3_adh2_ada_pMB1_AmpR (Plasmid EUPp_06)*	Investigating the order of EUP genes in one operon
PthrC3_H	*PthrC3_adh2_pMB1_AmpR (Plasmid EUPp_07)*	Investigating expression of single gene in EUP
PthrC3_A	*PthrC3_ada_pMB1_AmpR (Plasmid EUPp_08)*	Investigating expression of single gene in EUP
PgyrA_AH	*PgyrA_ada_adh2_pMB1_AmpR (Plasmid EUPp_09)*	Enhancing EUP by using stronger promoter
PthrC3_AH_ΔaldB*	*Plasmid EUPp_04*	Testing EUP in a *ΔaldB* strain
PgyrA_AH_Δpta **	*PgyrA_ada_adh2_pMB1_AmpR (Plasmid EUPp_09)*	Testing EUP in *Δpta* strain
PthrC325_phaCAB	*PthrC325_phaCAB_pAC_ChlR (Plasmid PHBp_01)*	Producing PHB from ethanol
PHB_PgyrA_AH	*Plasmid PHBp_01, Plasmid EUPp_09*	Producing PHB from ethanol
Prenol_PgyrA_AH***	*LacIT7p_hmgs_aibAB_T7p_Cbaid _liuC_Ecald _PgyrA_ada_adh2_pMB1_AmpR (Plasmid EUPp+IPAp), LacIT7p_atoB _pAC_SpecR (Plasmid atoBp)*	Producing Prenol from ethanol

MG1655_DE3 *(ΔrecA, ΔendA, DE3)* was used as the parent strain by default. The parent strain marked by * was **MG1655_DE3_ΔaldB** *(ΔrecA, ΔendA, ΔaldB, DE3)*. The parent strain marked by ** was **MG1655_DE3_ Δpta** *(ΔrecA, ΔendA, Δpta, DE3)*. The parent strain marked by *** was **BL21_DE3** (New England Biolabs, C2527H). AmpR: ampicilin resistance. ChlR: chlororamphanicol resistance. SpecR: spectinomycin resistance.

$(NH_4)_2HPO_4$, 0.0084 g/L EDTA, 0.0025 g/L $CoCl_2$, 0.015 g/L $MnCl_2$, 0.0015 g/L $CuCl_2$, 0.003 g/L H_3BO_3, 0.0025 g/L Na_2MoO_4, 0.008 g/L Zn $(CH_3COO)_2$, 0.06 g/L Fe(III) citrate, 1.3 g/L $MgSO_4$. Antibiotics (50 μg/mL ampicillin, 50 μg/mL spectinomycin, and/or 35 μg/mL chloramphenicol) were added according to Table 1, and pH was adjusted to 7 by using 400 g/L sodium hydroxide solution. 10 g/L ethanol was added as carbon source. Complete Supplement Mixture (CSM, Sunrise Science, 1001-100), amino acids or other carbon sources are additional components that were added as specified.

The composition of CSM: 10 mg/L adenine hemisulfate, 50 mg/L L-arginine, 80 mg/L L-aspartic acid, 20 mg/L L-histidine hydrochloride monohydrate, 50 mg/L L-isoleucine, 100 mg/L L-leucine, 50 mg/L L-lysine hydrochloride, 20 mg/L L-methionine, 50 mg/L L-phenylalanine, 100 mg/L L-threonine, 50 mg/L L-tryptophan, 50 mg/L L-tyrosine, 140 mg/L L-valine, and 20 mg/L uracil. All concentrations in this paragraph refer to working concentrations. The aspartate family contained 80 mg/L L-aspartate, 50 mg/L L-lysine, 100 mg/L L-threonine, 20 mg/L L-methionine, and 50 mg/L L-isoleucine. The pyruvate family contained 100 mg/L leucine and 140 mg/L L-valine. The aromatic family contained 50 mg/L L-tryptophan, 50 mg/L L-tyrosine, and 50 mg/L L-phenylalanine. The group labelled as "Others" contained 20 mg/L L-histidine and 50 mg/L L-arginine.

To culture the prenol-producing *E. coli* strain, the K3 medium supplemented with 10 g/L ethanol, 10 g/L tryptone, 5 g/L yeast extract (Clomburg et al., 2019) and proper amount of antibiotics was used. After inoculation, 0.01 mM or 0.1 mM isopropyl β-D-1-thiogalactopyranoside (IPTG) was added when the cell density (OD600) reached ~0.5 to induce the expression of the genes under the control of T7 promoter.

2.5. Enzyme activity assay

Crude cell extracts of **PthrC3_AH**, **PgyrA_AH**, and **MG1655_DE3** were used to measure activity of Ada and Adh2. The cells were cultured in LB medium overnight, and then inoculated into 25 mL of K3 medium at an initial OD600 of 0.02. Ethanol (10 g/L) was used as the sole carbon source of **PthrC3_AH** and of **PgyrA_AH**; Glucose (10 g/L) was used as sole carbon source of **MG1655_DE3**. The culture in 125 mL shake flasks were cultivated at 30 °C/220 rpm for 48 h. The grown cells were centrifuged at 4 °C/10,000 g for 5 min. The obtained cell pellets were washed twice by using Phosphate Buffered Saline (PBS, pH 7.4), and re-suspended in PBS to achieve OD600 = 50. A sonicator (QSONICA-Q500, USA) was employed for releasing intracellular proteins. The resulting solution was then centrifuged at 4 °C/10,000 g for 15 min. The obtained supernatant (referred as cell lysate below) was used to measure the enzyme activities. One unit (U) of enzyme activity was defined as producing 1 μmol of NADH per min. Normalized enzyme activity (U/g total proteins) was calculated by using the mass of the total proteins in cell lysate, which was determined by using the Bradford assay. Each reaction solution (1 mL) for measuring the activity of Adh2 contained 2 mM ethanol, 0.5 mM NAD^+, and cell lysate (the concentration of the total proteins of the cell lysate was adjusted to be 1 g/L, to ensure that the same amount of cell lysate was used in each reaction). Each reaction solution (1 mL) for measuring the activity of Ada contained 2 mM acetaldehyde, 0.5 mM NAD^+, 0.5 mM coenzyme A and cell lysate (the concentration of the total proteins of the cell lysate was 1 g/L). The reactions were incubated at 30 °C for 90 min, and the absorbance at 340 nm was measured after the incubation by using Varioskan LUX multimode microplate reader (Thermo Scientific). The readings of the reactions containing **MG1655_DE3** cell lysate were used as the baselines. After the baseline subtraction, the processed absorbance readings were used to calculate the amount of NADH produced during the 90 min, based on a calibration curve. Each experiment was conducted with triplicates.

2.6. Sampling and analysis of metabolites

The cell density was monitored by using Varioskan LUX multimode microplate reader (Thermo Scientific). Twenty microliters of cell suspension were diluted five times using deionized water, and the diluted cell suspension was loaded into a well in 96-well optical plate for measuring the absorbance at 600 nm. The reading was converted into standard OD600 reading by using a calibration curve. Ethanol consumption and acetate formation during the cell culture were monitored by using High-Performance Liquid Chromatography (HPLC). One hundred microliters of the culture medium were taken at each time point, followed by centrifugation at 12,000 rpm for 5 min. The obtained supernatant was then filtered using a 0.22 μm filter (Chemikalie Pte Ltd) and analyzed by HPLC (1260 Infinity series HPLC, Agilent) equipped with an Aminex HPX-87H column (300 X 7.8 mm, Bio-Rad). The flow rate was 0.7 mL/min, and the mobile phase was 5 mM H_2SO_4 aqueous solution. The column temperature was set at 50 °C. A refractive index detector (RID) was used for detecting the acetate and ethanol. HPLC grade ethanol and acetic acid were used to prepare standard solutions.

The quantification of PHB was based on a previously reported method (Tyo et al., 2010). Five hundred microliters of cell culture were collected and transferred to a safe-lock tube (Eppendorf) and centrifuged at 12,000 rpm for 2 min. The resulting cell pellet was washed twice with 1 mL of ice-cold deionized water. The cells were disrupted by vortexing in 200 μL of methanol and incubated at 60 °C for 15 min. The methanol was then removed by using a vacuum concentrator (Eppendorf) at 60 °C for 30 min. To hydrolyze PHB, two hundred microliters of 98% sulfuric acid was added to the dried cells, and incubated at 37 °C for 2 h,

followed by incubation at 95 °C for 40 min. The samples were then diluted 5 times using deionized water and centrifuged at 12,000 rpm for 5 min. The supernatant was filtered through a 0.22 μm filter for HPLC analysis, and the injection volume was 5 μL. A 25 min method was adopted for the quantification of crotonic acid (PHB was depolymerized and the monomer was dehydrated into crotonic acid). The rest of the HPLC conditions were the same as those described above. Commercially available crotonic acid (Sigma, 113018) was used to prepare standard solutions.

To quantify prenol produced by the engineered *E. coli* cells, nine hundred microliters of cell culture were collected and mixed with three hundred microliters of ethyl acetate, followed by vortexing at 30 °C for 30 min. The mixture was then centrifuged at 12,000 rpm for 5 min. One hundred microliters of the organic layer were transferred to a vial and analyzed by gas chromatography-mass spectrometry (GCMS, 5977B GC/MSD, Agilent Technologies). HP-5MS capillary column (30 m × 0.25 mm, 0.25 μm film thickness, Agilent Technologies) was used, with helium as the carrier gas. The following oven temperature program was carried out: 50 °C for 1 min, 50–100 °C at a rate of 5 °C/min, 100–300 °C at a rate of 75 °C/min, and 300 °C for 1 min. Five microliters of the sample were injected in a split injection mode (10:1). Commercially available prenol (Sigma, 162353) was used to prepare standard solutions.

2.7. Analysis of isotope distribution in phosphoenolpyruvate (PEP)

An Ultra Performance Liquid Chromatography (UPLC, Waters ACQUITY) linked with a Time-of-flight Mass Spectrometry (TOFMS, Bruker micrOTOF II) was used to analyze isotope distribution of PEP based on a previously reported method (Zhou et al., 2012). All the cultures were fed with 10 g/L of uniformly ^{13}C-labelled ethanol (Sigma, 427047). L-aspartate, the aspartate family amino acids or CSM were added to reach the final concentration of 1 g/L. A control without any supplementation was also included. The metabolites were extracted by adding 800 μL of methanol into 200 μL of cell suspension, vortexing the suspension for 10 min, and centrifuging at 12,000 rpm for 2 min. Then the supernatant was dried by using a vacuum concentrator at 60 °C for 30 min. The dried samples were resuspended in 100 μL of water. Five microliters of resuspended samples were injected, and a 12 min method was adopted for the quantification of PEP. In brief, the aqueous solution containing 15 mM acetic acid and 10 mM tributylamine was one mobile phase; methanol was the other mobile phase; the column was Poroshell 120 EC-C18 column (2.1 × 50 mm, 2.7 μm, Agilent Technologies). The mobile phase gradient program is summarized in **Supplementary Table 1**.

3. Results

3.1. Establishing EUP in E. coli

AdhE is an endogenous alcohol/aldehyde dehydrogenase in *E. coli*, which is responsible for ethanol production under oxygen-limited conditions. Wildtype *E. coli* cannot grow aerobically using ethanol as the sole carbon and energy source, possibly due to the low transcription rate of AdhE and its sensitivity to metal ion-catalyzed oxidation (Membrillo-Hernandez et al., 2000). In this study, we aim to establish an efficient ethanol utilization pathway in *E. coli*. It is well-known that *S. cerevisiae* can use an alcohol dehydrogenase (Adh2) to efficiently convert ethanol into acetaldehyde during its growth on ethanol (Thomson et al., 2005). Four acetaldehyde acylating dehydrogenases (MhpF, EutE, BhpJ and Ada) were also reported to convert acetaldehyde to acetyl-CoA in one step (Baker et al., 2012; Fischer et al., 2013; Kozak et al., 2014; Meadows et al., 2016). Based on these facts, we coupled each of the four genes (*mhpF, eutE, bhpJ* and *ada*) that encode acetaldehyde acylating dehydrogenase with *adh2* from *S. cerevisiae* to construct EUP in a *E. coli* strain derived from **MG1655** (Fig. 1a). In this EUP, acetyl-CoA can be synthesized from ethanol through a two-step enzymatic process without ATP consumption, while two NADH are generated per ethanol (Fig. 1a). As a comparison, *S. cerevisiae* uses a three-step pathway, in which acetaldehyde is oxidized into acetate, which is then activated into acetyl-CoA. The three-step pathway also regenerates two NADH per ethanol but consumes at least one ATP per ethanol. The essential cellular building blocks – including amino acids, lipids and nucleotides – can be produced from acetyl-CoA.

Each acetaldehyde dehydrogenase gene was clustered with *adh2* in an operon (Fig. 1b) under the control of an auto-inducible promoter PthrC3 (Anilionyte et al., 2018). Based on optical density at 600 nm, the growth of the engineered *E. coli* strains carrying the plasmids outperformed the parent strain that barely showed any cell growth (Fig. 1b) in a chemically defined medium with 10 g/L of ethanol as the sole carbon source. The *E. coli* carrying the plasmid with *ada* and *adh2* (PthrC_AH) generated substantially more biomass compared with other candidates (Fig. 1b), possibly due to Ada's higher expression level and/or specific activity when expressed in *E. coli*. A recent study also revealed that Ada was better than the other three acetaldehyde acylating dehydrogenases in *S. cerevisiae*, when they were used to enhance its cytosolic acetyl-CoA availability (Meadows et al., 2016).

We also constructed a *E. coli* strain expressing *ada* with a $NADP^+$-dependent alcohol dehydrogenase from *S. cerevisiae* (encoded by *adh 6*, Supplementary Fig. 1), with the hypothesis that cell growth was limited by NADPH supply. However, the strain reached lower cell density than PthrC_AH, invalidating the hypothesis.

To test if EUP requires both *ada* and *adh2*, we subsequently expressed the single enzyme of the EUP by using the plasmids carrying *ada* or *adh2* (Fig. 1c). The *E. coli* strain expressing only *adh2* did not grow in the medium that contained ethanol as the only carbon source (Fig. 1c), confirming the essentiality of *ada* in EUP. The OD600 of the strain that only overexpressed *ada* (**PthrC3_A**) reached ~0.8 (~25% of that of PthrC_AH, Fig. 1c), indicating that **PthrC3_A** expressed native alcohol dehydrogenases that were able to convert ethanol into acetaldehyde, although the conversion rate was lower than that of Adh2.

3.2. Increasing the ethanol utilization rate

We hypothesized that the ratio of reaction rate of the two steps in the EUP (catalyzed by Adh2 and Ada) was important for the cell to assimilate ethanol, as the intermediate acetaldehyde generated by EUP was toxic to the cell – the accumulated intermediate might inhibit the cells if the first reaction was too fast. Accordingly, we attempted to use several strategies to fine-tune the ratio of the expression level of *ada* and *adh2*.

We first shuffled *ada* and *adh2* in the operon. We previously placed *ada* in the first position of the operon in **PthrC3_AH**, which should lead to the higher expression level of *ada* – a gene would be transcribed at a higher level when placed at the beginning of an operon due to RNA polymerase premature termination and/or RNA degradation initiated from 3' end (Allen and Taatjes, 2015). When we swapped *ada* and *adh2* (**PthrC3_HA**, which should have a much lower ratio of Ada to Adh2), the final cell density achieved in the ethanol medium was reduced to 30% of that of **PthrC3_AH** (Fig. 2a). **PthrC3_AH** with *ada* at the first position consumed ~80% of the added ethanol (Fig. 2b), which was two times that of **PthrC3_HA**. We speculated that a larger ratio of Ada activity to Adh2 activity may improve ethanol utilization, so we decreased the expression level of *adh2* by replacing its ribosome binding site (RBS) with weaker RBSs (Supplementary Fig. 2) or mutating the core region of the original RBS (Supplementary Fig. 3). However, these strategies did not lead to a further increase in biomass formation or ethanol utilization, suggesting that the absolute expression level of Ada may be more important than the expression ratio.

Therefore, we continued to overexpress the *ada* and *adh2* by using the same gene order and the RBS used in PthrC3_AH. We replaced the PthrC3 promoter with a stronger promoter PgyrA (Anilionyte et al., 2018) to boost the protein expression (Fig. 2b). The new strain

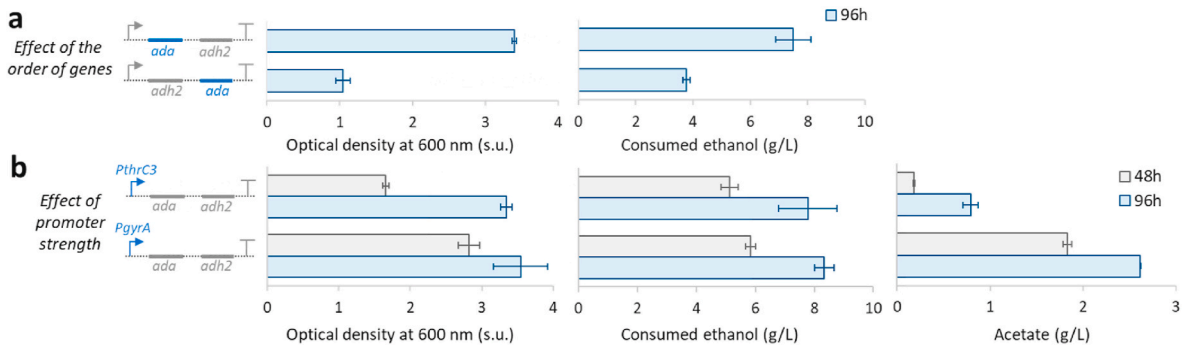

Fig. 2. Improving ethanol utilization rate in *E. coli* culture. (a) The effect of the order of two genes (*ada* and *adh2*) on cell growth and ethanol consumption. The strains used here are **PthrC3_AH** and **PthrC3_HA** (from top to bottom). Both *E. coli* strains used PthrC3 to overexpress the genes. (b) The effect of the strength of the promoter used to express *ada* and *adh2* on cell growth, ethanol consumption, and acetate formation. The strains used here are **PthrC3_AH** and **PgyrA_AH** (from top to bottom). Cells were cultured at 30 °C using 10 g/L of ethanol as the sole carbon source (no amino acids or nucleobases supplemented). The culture volume and vessel size: 10 mL of culture in 50 mL tubes. s.u.: standard unit. Error bars indicate standard error (n = 3).

(**PgyrA_AH**) had substantially higher activity of Adh2 and Ada than **PthrC3_AH** (enzyme activity: 2.06 ± 0.42 [**PthrC3_AH** Adh2]; 4.26 ± 0.48 [**PgyrA_AH** Adh2]; 3.01 ± 0.15 [**PthrC3_AH** Ada]; 5.95 ± 0.71 [**PgyrA_AH** Ada]; unit: U/g total proteins as defined in 2.5. Enzyme activity assay). Both *E. coli* strains consumed ethanol at a comparable rate and reached similar final cell densities, but PgyrA_AH grew substantially faster than **PthrC3_AH** (Fig. 2b). Interestingly, more than 2 g/L of acetate (Fig. 2b) was produced when PgyrA was used. As a comparison, the acetate concentration was only ~0.8 g/L in the culture of **PthrC3_AH**.

We attempted to improve the growth of **PgyrA_AH** on ethanol at a higher temperature. However, the cell growth of *E. coli* PgyrA_AH at 37 °C was much worse than that at 30 °C (Supplementary Fig. 4). It is possible that the expression of aldehyde dehydrogenase (Ada) and/or other enzymes involved in ethanol assimilation was better at 30 °C.

3.3. Coupling EUP with a downstream pathway

The acetate produced by **PgyrA_AH** might be produced from acetyl-CoA through the well-known carbon overflow reaction (Vemuri et al., 2006) involving phosphate acetyltransferase (Pta) and acetate kinase (AckA, Fig. 3a). Acetate may also be produced from the oxidation of acetaldehyde via the reaction catalyzed by a $NADP^+$-dependent aldehyde dehydrogenase (AldB, Fig. 3a) (Ho and Weiner, 2005). To understand how acetate was produced, we inactivated the acetaldehyde oxidation reaction by deleting *aldB* from the *E. coli*'s genome (Fig. 3a). This new *E. coli* strain (**PthrC3_AH_ΔaldB**) could not grow in the medium with ethanol as the sole carbon source (Supplementary Fig. 4), suggesting that at least some of the acetate we detected was generated by the one-step acetaldehyde oxidation reaction that can detoxify acetaldehyde and regenerate NADPH (Fig. 3a).

We then tested whether some of the acetate produced from ethanol was derived from acetyl-CoA (Fig. 3a). We deleted *pta* in the parent *E. coli* strain and introduced the Plasmid EUPp_09 into the *Δpta* strain. The cell growth and ethanol consumption profile of the new strain (**PgyrA_AH_Δpta**) were comparable to that of the control strain (**PgyrA_AH**, Supplementary Figs. 6a and b), but the acetate concentration in the culture of the new strain was substantially lower than that of the control strain at all the tested time points (Supplementary Fig. 6c), which supported that most of the acetate was derived from acetyl-CoA through the overflow mechanism.

To convert acetyl-CoA into a more valuable terminal product than

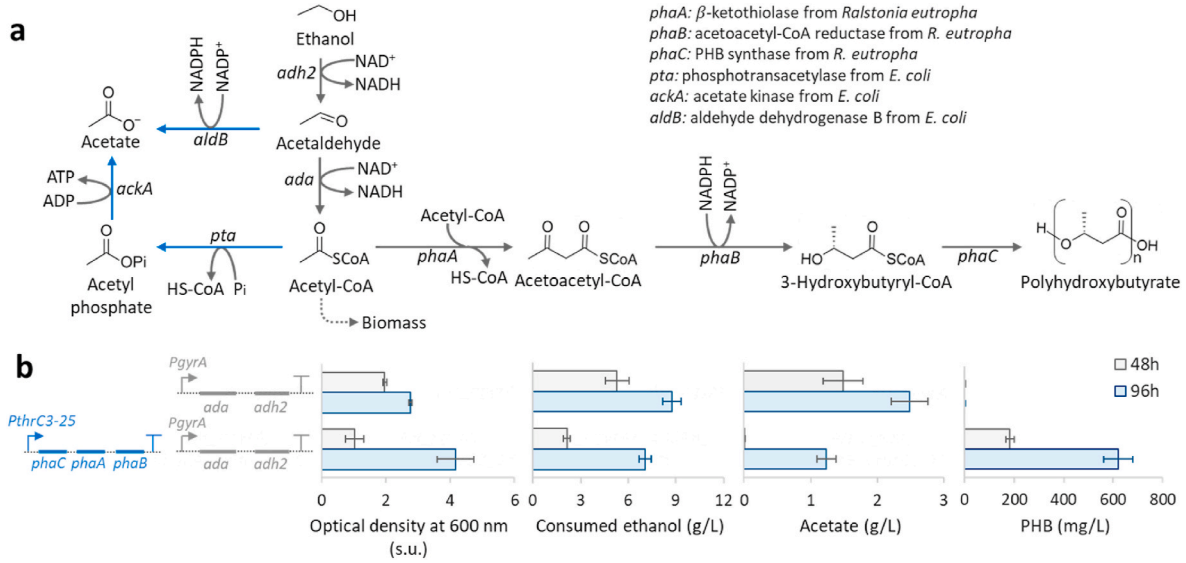

Fig. 3. Coupling PHB biosynthetic pathway with EUP in *E. coli*. (a) Biosynthetic pathway of acetate and PHB. (b) Effect of introducing the PHB-producing plasmid on OD600, ethanol consumption, acetate formation and PHB formation. The *E. coli* strains used here were **PgyrA_AH** and **PHB_PgyrA_AH** (from top to bottom). Cells were cultured at 30 °C using 10 g/L of ethanol as the sole carbon source (no amino acids supplemented). The culture volume and vessel size: 10 mL of culture in 50 mL tubes. s.u.: standard unit. Error bars indicate standard error (n = 3).

acetate, we introduced a downstream pathway that can convert acetyl-CoA into polyhydroxybutyrate (PHB). PHB belongs to the polyester class and is a useful product that may be used as biodegradable plastics for many industrial applications (Budde et al., 2011). The PHB biosynthesis starts from acetyl-CoA and exists in many microorganisms, in most of which two acetyl-CoA were condensed to one acetoacetyl-CoA that was reduced and subsequently polymerized (Kim et al., 2017). A plasmid (Plasmid PHBp_01) was constructed to express the genes *(phaA, phaB and phaC)* of these three steps under the control of a strong auto-inducible promoter PthrC3_25 (Anilionyte et al., 2018) (Fig. 3b). Plasmid PHBp_01 was introduced into **PgyrA_AH**, forming **PHB_PgyrA_AH**. Indeed, the concentration of acetate produced by **PHB_PgyrA_AH** was also substantially lower than that of **PgyrA_AH**, further supporting the hypothesis that the acetyl-CoA accumulated in **PgyrA_AH** causing the carbon overflow reaction (Fig. 3b). **PHB_PgyrA_AH** produced ~600 mg/L of PHB from 10 g/L of ethanol, proving that ethanol could be converted into acetyl-CoA derived compound via the EUP (Fig. 3b). We also confirmed that the same plasmids (PHBp_01 and EUPp_09) could enable other frequently used *E. coli* strains to produce PHB from ethanol (**Dh5**α and **BL21 DE3** were tested, Supplementary Fig. 5).

3.4. Improving the biosynthesis of PHB from ethanol

Ethanol needs to be transformed through glyoxylate shunt and gluconeogenesis (Phue and Shiloach, 2005) into many building blocks for biomass formation. We speculated that cell growth and PHB production could be limited by the biosynthesis of some building blocks (such as amino acids). Accordingly, we supplemented the medium with Complete Supplement Mixture (CSM) which is a mixture of amino acids and nucleobases. We first cultured the strain that could not synthesize PHB (**PgyrA_AH**) by using 10 g/L ethanol with or without 1 g/L of CSM supplementation. Although adding CSM did not improve specific growth rate, it almost doubled the final cell density (Supplementary Fig. 8), supporting that cell growth was limited by supply of certain building blocks. When 1 g/L of CSM was added to culture of the PHB-producing strain (**PHB_PgyrA_AH**), the PHB titer (1.1 g/L) was also almost doubled (PHB titer without CSM supplementation: 0.6 g/L; ethanol concentration under both conditions: 10 g/L; Fig. 4b).

To understand which amino acids were responsible for the improvement of PHB production, the amino acids in CSM were grouped into four groups based on their biosynthetic pathways (aromatic family, pyruvate family, aspartate family and others [Fig. 4a]; the concentration of each amino acid in a group was the same to that in CSM; the detailed composition of each amino acid family is listed in Section 2.1). We fed **PHB_PgryA_AH** with 10 g/L of ethanol and one group of amino acids. The strain supplemented with the aspartate family amino acids achieved the same level of PHB as the CSM supplementation (Fig. 4b), suggesting that this group of amino acids were mainly responsible for the beneficial effects of CSM in the previous experiment. Supplementing other families of amino acids did not increase PHB production (Fig. 4b). There could be two mechanisms by which the aspartate family of amino acids can contribute to the PHB production: (1) they may improve synthesis of the key enzymes involved in PHB production and biomass formation by providing the amino acids that were in short supply; (2) the amino acids may be catabolized and were transformed into monomer of PHB, providing extra carbon source for PHB synthesis.

To test if the added amino acids could be assimilated into the central metabolism, we used uniformly ^{13}C-labelled (U–^{13}C) ethanol and non-labelled amino acids to culture **PHB_PgyrA_AH**. When growing on ethanol or the aspartate family of amino acids, the cells have to use gluconeogenesis to generate metabolites to fuel the pentose phosphate pathway for making nucleotides and other building blocks. Phosphoenolpyruvate (PEP) is a key node intermediate in gluconeogenesis, which can be derived from pyruvate or oxaloacetate (Fig. 4a). We selected PEP as the model metabolite to study in this experiment. Since the primary carbon source we used was U–^{13}C ethanol (10 g/L), the carbon atoms in PEP should be primarily ^{13}C, resulting in PEP molecules that have substantially increased molecular weight (i.e., M3 and M2,

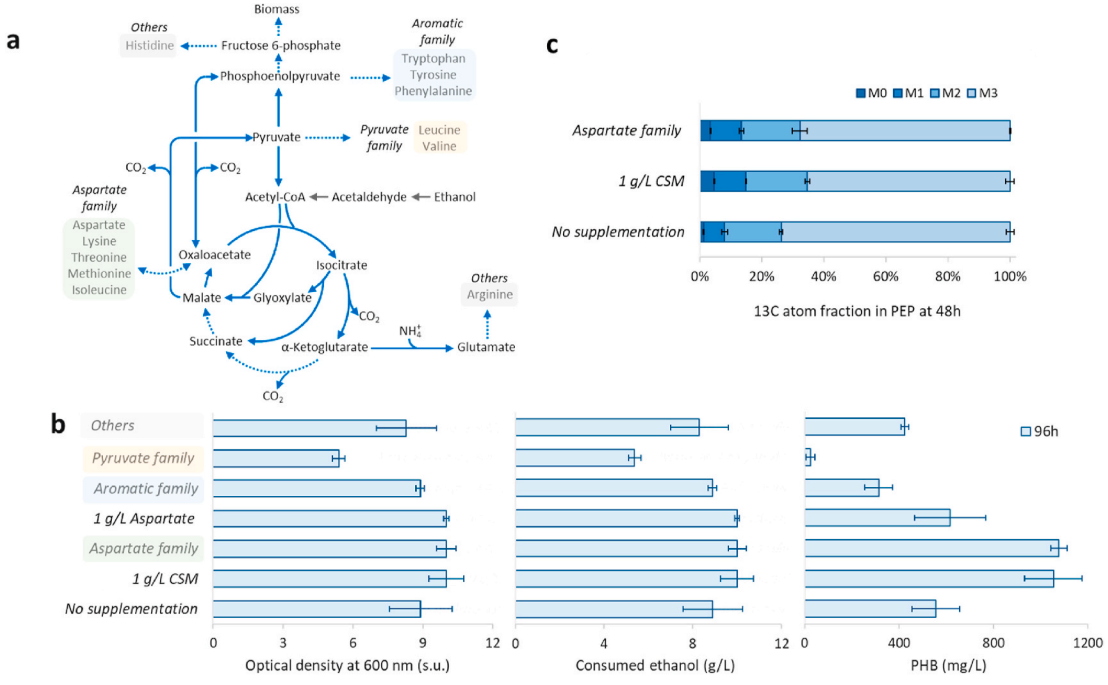

Fig. 4. Improvement of PHB production from ethanol by feeding low concentration of amino acids. (a) Key metabolic pathways related to cell growth on ethanol. (b) Effect of feeding amino acid(s) and/or nucleobases on OD600, ethanol consumption and PHB production. (c) Effect of amino acid and/or nucleobases supplementation on isotope distribution in PEP. Ethanol (10 g/L) was added under all the conditions. Amino acids and/or nucleobases were supplemented as labelled in the figure. Concentration of each amino acid in each group was the same to that in CSM. The detailed compositions are listed in Section 2.4. Cells were cultured in the K3 medium at 30 °C. Culture volume and vessel size: 10 mL of culture in 50 mL culture tubes when non-labelled ethanol was used; 1 mL culture in 14 mL culture tubes when U–^{13}C ethanol was used. The samples were collected at 48 h. s.u.: standard unit. Error bars indicate standard error (n = 3).

here M3 refers to M+3 and M is the molecular weight when all carbon atoms are ^{12}C; PEP has three carbon atoms). If ^{12}C atoms in non-labelled amino acids were assimilated into central metabolism, we would expect to see a substantial increase in M0 fraction of PEP. The experimental results show that the fraction of M0 indeed increased from 1% to 5% when aspartate family amino acids or 1 g/L of CSM were added (Fig. 4c), implying that some of these amino acids were indeed catabolized but the flux was still much smaller than that from ethanol (the fraction of M3 was still more than 60% when the amino acids were supplemented). It is unclear why the fraction of M1 and M2 was together more than 20% when U–^{13}C ethanol was the sole carbon source. One possible mechanism is assimilation of ^{12}C CO_2 catalyzed by phosphoenolpyruvate carboxylase.

3.5. Producing prenol from ethanol

Isoprenoids, a large family of natural products (at least 55,000 known examples), have been used in many applications, such as being used as flavor and fragrance agents, and plant hormones (Barkovich and Liao, 2001; Luo et al., 2015). There are three isoprenoid biosynthetic pathways: the mevalonate (MVA) pathway (Ro et al., 2006), the 2-C-methyl-D-erythritol 4-phosphate (MEP) pathway (Li et al., 2012) and isoprenoid alcohol (IPA) pathway (Clomburg et al., 2019). The MVA pathway and IPA can be coupled with EUP for isoprenoid production, because both MVA and IPA pathways were linked with central metabolism by acetyl-CoA.

We decided to prove that the EUP can be extended to produce prenol, which is a key intermediate in IPA. The results would support that EUP can be used to produce different classes of acetyl-CoA derived compounds. We used two plasmids to reconstruct the pathway from ethanol to prenol (Fig. 5b) and tested the plasmids in two *E. coli* strains: **MG1655_DE3** and **BL21_DE3**. Only the **BL21_DE3** derived strain (**Prenol_PgyrA_AH**) produced a detectable amount of prenol (24 mg/L from 10 g/L of ethanol, 10 g/L tryptone and 5 g/L yeast extract Fig. 5c–e). We added tryptone and yeast extract because they were used by the study which first reported the prenol production in *E. coli* (Clomburg et al., 2019). No prenol was produced when 10 g/L tryptone and 5 g/L yeast extract were used without ethanol in our study (Supplementary Table 2), suggesting that the produced prenol could be derived from ethanol. The strain was also cultivated in a glucose medium (10 g/L glucose) as a control, and it produced a similar amount of prenol (21 mg/L). The strain achieved similar final cell density in the two media and consumed most of the carbon sources by 48 h. The *E. coli* strain, however, produced much less acetate in the ethanol medium than the glucose medium (the acetate concentrations were 1.1 g/L and 6.4 g/L for the ethanol and glucose medium respectively, Fig. 5c), suggesting that the acetate overflow pathway was much less active when the cells grew on ethanol. The results obtained demonstrated the feasibility of converting ethanol into prenol and thus provided the opportunity of producing isoprenoids from ethanol-derived prenol. We expect that a higher prenol titer would be obtained in both **BL21_DE3** and **MG1655_DE3** derived strains when this pathway is optimized. Very recently, a new, redox balanced isopentanol biosynthetic pathway was developed (Eiben et al., 2020). The engineered *E. coli* produced 80 mg/L of isopentanol by using glucose at the microaerobic condition with mixed acids produced, providing another possibility to link the EUP developed in this study with prenol.

4. Discussion

The EUP developed in this study provides a pathway to convert ethanol into acetyl-CoA derived compounds in *E. coli*. The ethanol consumption was improved by expressing *ada* and *adh2* in a specific order (*ada-adh2*) by using a constitutive promoter (PgyrA). The EUP was able to produce 1.1 g/L of PHB when 10 g/L of ethanol and 1 g/L of aspartate family amino acids were fed. We also engineered *E. coli* strain to produce 24 mg/L of prenol from 10 g/L of ethanol in 48 h, supporting

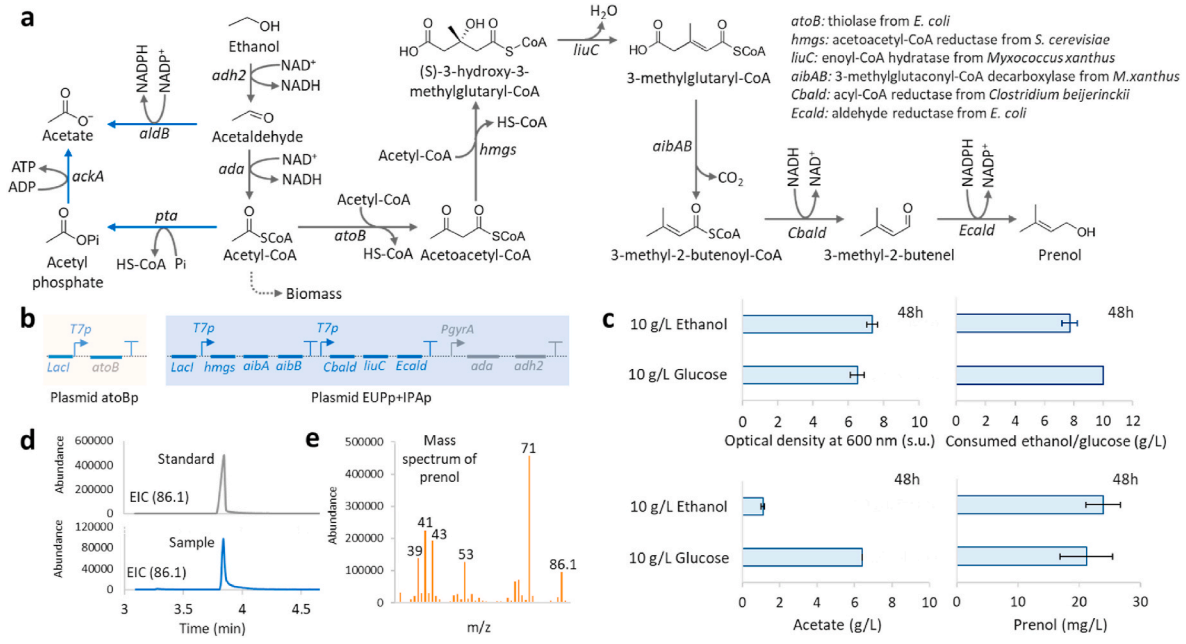

Fig. 5. Production of prenol from ethanol using the *E. coli*. (a) Metabolic pathway of converting ethanol into prenol. (b) Plasmids constructed to convert ethanol to prenol. Plasmid atoBp containing one operon was constructed with a backbone that contained SpecR (antibiotic resistance) and pAC (replication origin). Plasmid EUP+IPAp carrying three operons was constructed with a backbone that contained AmpR (antibiotic resistance) and pMB1 (replication origin). (c) Comparison between using ethanol and using glucose as the major carbon source for prenol production. Cell growth, substrate consumption, acetate formation and prenol production were monitored. Cell culture was done in the K3 medium at 30 °C with 10 g/L of ethanol or glucose as a carbon source with 10 g/L of tryptone and 5 g/L of yeast extract. The expression of the genes under the control of T7 promoter was induced by using 0.01 mM IPTG (when 10 g/L ethanol was used) or 0.1 mM IPTG (when 10 g/L glucose was used) when OD600 reached 0.5–0.6. (d) Extracted Ion Chromatogram of standard and sample (obtained by using ethanol as the main carbon source, m/z = 86.1). (e) Mass spectrum of the prenol derived from ethanol. s.u.: standard unit. Error bars indicate standard error (n = 3).

the feasibility of producing different families of acetyl-CoA derived compounds. With EUP, many other important acetyl-CoA derived compounds could theoretically be synthesized from ethanol. Malonyl-CoA is an important building block that can be derived from acetyl-CoA. Malonyl-CoA can be used to synthesize biopolymers (e.g., polyhydroxypropionate) (Jiang et al., 2009), fatty acids (Liu et al., 2015), polyketides (Wattanachaisaereekul et al., 2008) and flavonoids (Zha et al., 2009).

Two molecules of NADH would be generated when one molecule of ethanol was converted into acetyl-CoA, and need to be oxidized, possibly through respiration, for continuing ethanol assimilation. In such case, oxygen would play an important role in ethanol assimilation as cells require oxygen as electron acceptors during respiration. We investigated the effect of oxygen supply on cell growth when ethanol was used as the sole carbon source. As expected, under anaerobic condition, **PthrC3_AH** cannot consume most of the ethanol added into the medium (Supplementary Fig. 6), formed less quantity of biomass and converted most of the consumed ethanol into acetate (2 g/L). In order to test if oxygen supply limited cell growth on ethanol, we scaled up the culture volume from 10 mL to 25 mL and used 125 mL shake flasks instead of 50 mL culture tubes. Oxygen supply was expected to be better under the shake flask condition. **PgyrA_AH** and **PHB_PgyrA_AH** were tested under this new condition. Ethanol (10 g/L) was used as the sole carbon source without CSM supplementation (Supplementary Fig. 11). Both strains had similar growth profiles when grown in the test tubes and shake flasks, suggesting that the growth was not limited by oxygen supply under the culture tube condition.

Ethanol is known to inhibit *E. coli* growth (Zhou et al., 2015). We tested a range of initial ethanol concentrations (10 g/L, 15 g/L, 20 g/L, 30 g/L and 40 g/L). Although a similar final cell density was achieved by 96 h, **PgyrA_AH** indeed grew slower at higher ethanol concentration (Supplementary Fig. 9). The inhibitory effect of ethanol on the cell growth can be overcome by using process engineering. For example, a low initial ethanol concentration could be used, and ethanol could be added to a stirred tank bioreactor by using a pump. The feeding rate can be controlled to achieve an ethanol-limited condition, where the ethanol centration in the medium is small.

Recently a three-step ethanol assimilation pathway (similar to the one working in *S. cerevisiae*) has been introduced into *E. coli* (Cao et al., 2020). However, the use of ethanol as the sole carbon source was not achieved in the study (Cao et al., 2020). The process needed to use 1 g/L of glucose to generate biomass before adding ethanol into the medium as the substrate. As a comparison, the strain in our study grew on ethanol as sole carbon source. Amino acid supplementation was shown to increase the rate of ethanol assimilation, but it was not needed for the *E. coli* strain to grow on ethanol as sole carbon source. Besides this critical point, our study is also different from Cao et al., (2020) in the following ways: a) a much larger amount of ethanol was assimilated in our study (8 g/L in our study without amino acid supplementation; 2.2 g/L in their study); b) Gram per liter product titer was achieved in our study (1.2 g/L PHB) while they did not report their product titer; c) a shorter and more ATP-efficient pathway was used in our study.

Laboratory adaptive evolution was recently used to improve growth of an *E. coli* **MG1655** strain when ethanol was used as a carbon source (Eremina et al., 2019). The parent *E. coli* strain carried a mutated alcohol/aldehyde dehydrogenase, which allowed converting ethanol into acetaldehyde. The evolved *E. coli* strain contained a mutation in an RNA polymerase subunit which positively increased the cell growth on ethanol (Eremina et al., 2019). Although the biomass achieved by the evolved *E. coli* strain was comparable with that obtained with the EUP in this study, it was unknown if the evolved *E. coli* strain was able to efficiently produce acetyl-CoA derived products from ethanol. The best *E. coli* strain developed in our study may be further improved by introducing the mutation found by Eremina et al. or through an independent adaptive evolution, by which the ethanol tolerance, gluconeogenesis, and/or ATP supply from the TCA cycle may be tuned.

CRediT authorship contribution statement

Hong Liang: Conceptualization, Methodology, Investigation, Formal analysis, Writing - original draft. **Xiaoqiang Ma:** Methodology, Investigation, Formal analysis. **Wenbo Ning:** Investigation. **Yurou Liu:** Investigation. **Anthony J. Sinskey:** Supervision, Funding acquisition. **Gregory Stephanopoulos:** Conceptualization, Methodology, Supervision, Funding acquisition. **Kang Zhou:** Conceptualization, Methodology, Supervision, Writing - review & editing, Funding acquisition.

Declaration of competing interest

The authors declare no conflict of interest.

Acknowledgment

This work was supported by Disruptive & Sustainable Technologies for Agricultural Precision Grant (R-279-000-531-592). We thank Professor Kristala Jones Prather (Massachusetts Institute of Technology) for her advice and providing MG1655_DE3.

Appendix A. Supplementary data

Supplementary data to this article can be found online at https://doi.org/10.1016/j.ymben.2020.11.010.

References

Allen, B.L., Taatjes, D.J., 2015. The Mediator complex: a central integrator of transcription. Nat. Rev. Mol. Cell Biol. 16, 155–166.
Anilionyte, O., Liang, H., Ma, X., Yang, L., Zhou, K., 2018. Short, auto-inducible promoters for well-controlled protein expression in Escherichia coli. Appl. Microbiol. Biotechnol. 102, 7007–7015.
Arán-Ais, R.M., Scholten, F., Kunze, S., Rizo, R., Roldan Cuenya, B., 2020. The role of in situ generated morphological motifs and Cu(i) species in C2+ product selectivity during CO2 pulsed electroreduction. Nature Energy 5, 317–325.
Baker, P., Carere, J., Seah, S.Y., 2012. Substrate specificity, substrate channeling, and allostery in BphJ: an acylating aldehyde dehydrogenase associated with the pyruvate aldolase BphI. Biochemistry 51, 4558–4567.
Bang, J., Lee, S.Y., 2018. Assimilation of formic acid and CO2 by engineered Escherichia coli equipped with reconstructed one-carbon assimilation pathways. Proc. Natl. Acad. Sci. U. S. A. 115, E9271–E9279.
Barkovich, R., Liao, J.C., 2001. Metabolic engineering of isoprenoids. Metab. Eng. 3, 27–39.
Budde, C.F., Riedel, S.L., Hubner, F., Risch, S., Popovic, M.K., Rha, C., Sinskey, A.J., 2011. Growth and polyhydroxybutyrate production by Ralstonia eutropha in emulsified plant oil medium. Appl. Microbiol. Biotechnol. 89, 1611–1619.
Cao, Y., Mu, H., Guo, J., Liu, H., Zhang, R., Liu, W., Xian, M., Liu, H., 2020. Metabolic engineering of Escherichia coli for the utilization of ethanol. J Biol Res (Thessalon). 27, 1.
Clomburg, J.M., Qian, S., Tan, Z., Cheong, S., Gonzalez, R., 2019. The isoprenoid alcohol pathway, a synthetic route for isoprenoid biosynthesis. Proc. Natl. Acad. Sci. U. S. A. 116, 12810–12815.
Eiben, C.B., Tian, T., Thompson, M.G., Mendez-Perez, D., Kaplan, N., Goyal, G., Chiniquy, J., Hillson, N.J., Lee, T.S., Keasling, J.D., 2020. Adenosine triphosphate and carbon efficient route to second generation biofuel isopentanol. ACS Synth. Biol.
Eremina, N.S., Slivinskaya, E.A., Yampolskaya, T.A., Rybak, K.V., Altman, I.B., Ptitsyn, L. R., Stoynova, N.V., 2019. Adaptive evolution of Escherichia coli K-12 MG1655 grown on ethanol and glycerol. Appl. Biochem. Microbiol. 54, 793–799.
Fischer, B., Boutserin, S., Mazon, H., Collin, S., Branlant, G., Gruez, A., Talfournier, F., 2013. Catalytic properties of a bacterial acylating acetaldehyde dehydrogenase: evidence for several active oligomeric states and coenzyme A activation upon binding. Chem. Biol. Interact. 202, 70–77.
Fuhrer, T., Fischer, E., Sauer, U., 2005. Experimental identification and quantification of glucose metabolism in seven bacterial species. J. Bacteriol. 187, 1581–1590.
Gurudayal, G., Bullock, J., Srankó, D.F., Towle, C.M., Lum, Y., Hettick, M., Scott, M.C., Javey, A., Ager, J., 2017. Efficient solar-driven electrochemical CO2 reduction to hydrocarbons and oxygenates. Energy Environ. Sci. 10, 2222–2230.
Ho, K.K., Weiner, H., 2005. Isolation and characterization of an aldehyde dehydrogenase encoded by the aldB gene of Escherichia coli. J. Bacteriol. 187, 1067–1073.
Jiang, X., Meng, X., Xian, M., 2009. Biosynthetic pathways for 3-hydroxypropionic acid production. Appl. Microbiol. Biotechnol. 82, 995–1003.
Jiang, Y., Chen, B., Duan, C., Sun, B., Yang, J., Yang, S., Kelly, R.M., 2015. Multigene editing in the Escherichia coli genome via the CRISPR-Cas9 system. Appl. Environ. Microbiol. 81, 2506–2514.

Kim, Y.J., Choi, S.Y., Kim, J., Jin, K.S., Lee, S.Y., Kim, K.J., 2017. Structure and function of the N-terminal domain of Ralstonia eutropha polyhydroxyalkanoate synthase, and the proposed structure and mechanisms of the whole enzyme. Biotechnol. J. 12.

Kozak, B.U., van Rossum, H.M., Benjamin, K.R., Wu, L., Daran, J.M., Pronk, J.T., van Maris, A.J., 2014. Replacement of the Saccharomyces cerevisiae acetyl-CoA synthetases by alternative pathways for cytosolic acetyl-CoA synthesis. Metab. Eng. 21, 46–59.

Li, F., Li, Y.C., Wang, Z., Li, J., Nam, D.-H., Lum, Y., Luo, M., Wang, X., Ozden, A., Hung, S.-F., Chen, B., Wang, Y., Wicks, J., Xu, Y., Li, Y., Gabardo, C.M., Dinh, C.-T., Wang, Y., Zhuang, T.-T., Sinton, D., Sargent, E.H., 2019. Cooperative CO2-to-ethanol conversion via enriched intermediates at molecule–metal catalyst interfaces. Nature Catalysis 3, 75–82.

Li, H., Opgenorth, P.H., Wernick, D.G., Rogers, S., Wu, T.Y., Higashide, W., Malati, P., Huo, Y.X., Cho, K.M., Liao, J.C., 2012. Integrated electromicrobial conversion of CO2 to higher alcohols. Science 335, 1596.

Lian, J., Si, T., Nair, N.U., Zhao, H., 2014. Design and construction of acetyl-CoA overproducing Saccharomyces cerevisiae strains. Metab. Eng. 24, 139–149.

Liu, D., Xiao, Y., Evans, B.S., Zhang, F., 2015. Negative feedback regulation of fatty acid production based on a malonyl-CoA sensor-actuator. ACS Synth. Biol. 4, 132–140.

Liu, H., Marsafari, M., Wang, F., Deng, L., Xu, P., 2019.

Luo, M., Wang, Z., Li, Y.C., Li, J., Li, F., Lum, Y., Nam, D.H., Chen, B., Wicks, J., Xu, A., Zhuang, T., Leow, W.R., Wang, X., Dinh, C.T., Wang, Y., Wang, Y., Sinton, D., Sargent, E.H., 2019. Hydroxide promotes carbon dioxide electroreduction to ethanol on copper via tuning of adsorbed hydrogen. Nat. Commun. 10, 5814.

Luo, Y., Li, B.Z., Liu, D., Zhang, L., Chen, Y., Jia, B., Zeng, B.X., Zhao, H., Yuan, Y.J., 2015. Engineered biosynthesis of natural products in heterologous hosts. Chem. Soc. Rev. 44, 5265–5290.

Ma, W., Xie, S., Liu, T., Fan, Q., Ye, J., Sun, F., Jiang, Z., Zhang, Q., Cheng, J., Wang, Y., 2020. Electrocatalytic reduction of CO2 to ethylene and ethanol through hydrogen-assisted C–C coupling over fluorine-modified copper. Nature Catalysis.

Ma, X., Liang, H., Cui, X., Liu, Y., Lu, H., Ning, W., Poon, N.Y., Ho, B., Zhou, K., 2019. A standard for near-scarless plasmid construction using reusable DNA parts. Nat. Commun. 10, 3294.

Meadows, A.L., Hawkins, K.M., Tsegaye, Y., Antipov, E., Kim, Y., Raetz, L., Dahl, R.H., Tai, A., Mahatdejkul-Meadows, T., Xu, L., Zhao, L., Dasika, M.S., Murarka, A., Lenihan, J., Eng, D., Leng, J.S., Liu, C.L., Wenger, J.W., Jiang, H., Chao, L., Westfall, P., Lai, J., Ganesan, S., Jackson, P., Mans, R., Platt, D., Reeves, C.D., Saija, P.R., Wichmann, G., Holmes, V.F., Benjamin, K., Hill, P.W., Gardner, T.S., Tsong, A.E., 2016. Rewriting yeast central carbon metabolism for industrial isoprenoid production. Nature 537, 694–697.

Membrillo-Hernandez, J., Echave, P., Cabiscol, E., Tamarit, J., Ros, J., Lin, E.C., 2000. Evolution of the adhE gene product of Escherichia coli from a functional reductase to a dehydrogenase. Genetic and biochemical studies of the mutant proteins. J. Biol. Chem. 275, 33869–33875.

Phue, J.N., Shiloach, J., 2005. Impact of dissolved oxygen concentration on acetate accumulation and physiology of E. coli BL21, evaluating transcription levels of key genes at different dissolved oxygen conditions. Metab. Eng. 7, 353–363.

Pontrelli, S., Fricke, R.C.B., Teoh, S.T., Lavina, W.A., Putri, S.P., Fitz-Gibbon, S., Chung, M., Pellegrini, M., Fukusaki, E., Liao, J.C., 2018. Metabolic repair through emergence of new pathways in Escherichia coli. Nat. Chem. Biol. 14, 1005–1009.

Protzko, R.J., Latimer, L.N., Martinho, Z., de Reus, E., Seibert, T., Benz, J.P., Dueber, J.E., 2018. Engineering Saccharomyces cerevisiae for co-utilization of D-galacturonic acid and D-glucose from citrus peel waste. Nat. Commun. 9, 5059.

Ren, D., Deng, Y., Handoko, A.D., Chen, C.S., Malkhandi, S., Yeo, B.S., 2015. Selective electrochemical reduction of carbon dioxide to ethylene and ethanol on copper(I) oxide catalysts. ACS Catal. 5, 2814–2821.

Ro, D.K., Paradise, E.M., Ouellet, M., Fisher, K.J., Newman, K.L., Ndungu, J.M., Ho, K.A., Eachus, R.A., Ham, T.S., Kirby, J., Chang, M.C., Withers, S.T., Shiba, Y., Sarpong, R., Keasling, J.D., 2006. Production of the antimalarial drug precursor artemisinic acid in engineered yeast. Nature 440, 940–943.

Robak, K., Balcerek, M., 2018. Review of second generation bioethanol production from residual biomass. Food Technol. Biotechnol. 56, 174–187.

Sakimoto, K.K., Zhang, S.J., Yang, P., 2016. Cysteine-cystine photoregeneration for oxygenic photosynthesis of acetic acid from CO2 by a tandem inorganic-biological hybrid system. Nano Lett. 16, 5883–5887.

Song, Y., Peng, R., Hensley, D.K., Bonnesen, P.V., Liang, L., Wu, Z., Meyer, H.M., Chi, M., Ma, C., Sumpter, B.G., Rondinone, A.J., 2016. High-Selectivity electrochemical conversion of CO2to ethanol using a copper nanoparticle/N-doped graphene electrode. Chemistry 1, 6055–6061.

Thomson, J.M., Gaucher, E.A., Burgan, M.F., De Kee, D.W., Li, T., Aris, J.P., Benner, S.A., 2005. Resurrecting ancestral alcohol dehydrogenases from yeast. Nat. Genet. 37, 630–635.

Ting, L.R.L., Piqué, O., Lim, S.Y., Tanhaei, M., Calle-Vallejo, F., Yeo, B.S., 2020. Enhancing CO2 electroreduction to ethanol on copper–silver composites by opening an alternative catalytic pathway. ACS Catal. 10, 4059–4069.

Tyo, K.E., Fischer, C.R., Simeon, F., Stephanopoulos, G., 2010. Analysis of polyhydroxybutyrate flux limitations by systematic genetic and metabolic perturbations. Metab. Eng. 12, 187–195.

Vemuri, G.N., Altman, E., Sangurdekar, D.P., Khodursky, A.B., Eiteman, M.A., 2006. Overflow metabolism in Escherichia coli during steady-state growth: transcriptional regulation and effect of the redox ratio. Appl. Environ. Microbiol. 72, 3653–3661.

Wattanachaisaereekul, S., Lantz, A.E., Nielsen, M.L., Nielsen, J., 2008. Production of the polyketide 6-MSA in yeast engineered for increased malonyl-CoA supply. Metab. Eng. 10, 246–254.

Wendisch, V.F., Brito, L.F., Gil Lopez, M., Hennig, G., Pfeifenschneider, J., Sgobba, E., Veldmann, K.H., 2016. The flexible feedstock concept in Industrial Biotechnology: metabolic engineering of Escherichia coli, Corynebacterium glutamicum, Pseudomonas, Bacillus and yeast strains for access to alternative carbon sources. J. Biotechnol. 234, 139–157.

Whitaker, W.B., Jones, J.A., Bennett, R.K., Gonzalez, J.E., Vernacchio, V.R., Collins, S.M., Palmer, M.A., Schmidt, S., Antoniewicz, M.R., Koffas, M.A., Papoutsakis, E.T., 2017. Engineering the biological conversion of methanol to specialty chemicals in Escherichia coli. Metab. Eng. 39, 49–59.

Woolston, B.M., King, J.R., Reiter, M., Van Hove, B., Stephanopoulos, G., 2018. Improving formaldehyde consumption drives methanol assimilation in engineered E. coli. Nat. Commun. 9, 2387.

Yadav, R.K., Baeg, J.O., Oh, G.H., Park, N.J., Kong, K.J., Kim, J., Hwang, D.W., Biswas, S. K., 2012. A photocatalyst-enzyme coupled artificial photosynthesis system for solar energy in production of formic acid from CO2. J. Am. Chem. Soc. 134, 11455–11461.

Zha, W., Rubin-Pitel, S.B., Shao, Z., Zhao, H., 2009. Improving cellular malonyl-CoA level in Escherichia coli via metabolic engineering. Metab. Eng. 11, 192–198.

Zhou, K., Qiao, K., Edgar, S., Stephanopoulos, G., 2015. Distributing a metabolic pathway among a microbial consortium enhances production of natural products. Nat. Biotechnol. 33, 377–383.

Zhou, K., Zou, R., Stephanopoulos, G., Too, H.P., 2012. Metabolite profiling identified methylerythritol cyclodiphosphate efflux as a limiting step in microbial isoprenoid production. PLoS One 7, e47513.